ARTICLE IN PRESS

Physica A ▮ (▮▮▮▮) ▮▮▮–▮▮▮

Contents lists available at ScienceDirect

Physica A

journal homepage: www.elsevier.com/locate/physa

Scattering in thick multifractal clouds, Part II: Multiple scattering

S. Lovejoy [a,*], B.P. Watson [b], Y. Grosdidier [a], D. Schertzer [c]

[a] Department of Physics, McGill University, 3600 University Street, Montreal, Que. H3A 2T8, Canada

[b] Department of Physics, St. Lawrence University, Canton, NY 13617, USA

[c] CEREVE, Ecole Nationale des Ponts et Chaussées, 6-8, avenue Blaise Pascal, Cité Descartes, 77455 MARNE-LA-VALLEE Cedex, France

ARTICLE INFO

Article history:
Received 1 October 2008
Received in revised form 1 May 2009
Available online xxxx

Keywords:
Light scattering
Multifractal
Clouds
Turbulence
Transport in disordered media

ABSTRACT

In Part I of this paper, we developed asymptotic approximations for single photon scattering in thick, highly heterogeneous, "Log-Lévy" multifractal clouds. In Part II, theoretical multiple scattering predictions are numerically tested using Monte Carlo techniques, which show that, due to long range correlations, the photon paths are "subdiffusive" with the corresponding fractal dimensions tending to increase slowly with mean optical thickness. We develop reasonably accurate statistical relations between N scatter statistics in thick clouds and single scatter statistics in thin clouds. This is explored further using discrete angle radiative transfer (DART) approach in which the radiances decouple into non-interacting families with only four (for 2-D clouds) radiance directions each. Sparse matrix techniques allow for rapid and extremely accurate solutions for the transfer; the accuracy is only limited by the spatial discretization.

By "renormalizing" the cloud density, we relate the mean transmission statistics to those of an equivalent homogeneous cloud. This simple idea is remarkably effective because two complicating effects act in contrary directions: the "holes" which lead to increased single scatter transmission and the tendency for multiply scattered photons to become "trapped" in optically dense regions, thus decreasing the overall transmission.

1. Multiple scattering and non-conservative multifractals

From the point of view of applications, the single scattering results of Part I have severe limitations. First, it is not obvious how those calculations are relevant to multiple scattered radiation in thick clouds. In addition, even for single scattering, it is not clear that the results will be relevant in non-conservative clouds in which the cloud density is related to the (scale by scale) conservative multifractal fluxes by a fractional integration as outlined in Section 2.1 of Part I. We mentioned that the Corrsin–Obukov law for passive scalar advection yields $H = 1/3$ and $\varphi = \chi^{\frac{1}{2}}\varepsilon^{-\frac{1}{6}}$ where χ is the passive scalar variance flux and ε is the energy flux. Observations of aerosols [1–4] and cloud liquid water [5,6] show that in the horizontal H is indeed close to $1/3$. Unfortunately, the analytic treatment of the statistics of the fractionally integrated flux (FIF) model with $H \neq 0$ is too difficult; the same is true of extending the above directly to multiple scattering since successive scatters are strongly correlated. We will therefore turn to numerical simulations.

Fig. 1a and b show 12 multifractal simulations on 512^2grids of the conserved flux φ (i.e. $H = 0$) and their fractional integration by $H = 1/3$ respectively, showing the large realization-to-realization variability as well as the smoothing

* Corresponding author.
E-mail address: lovejoy@physics.mcgill.ca (S. Lovejoy).

0378-4371/$ – see front matter © 2009 Elsevier B.V. All rights reserved.
doi:10.1016/j.physa.2009.05.037

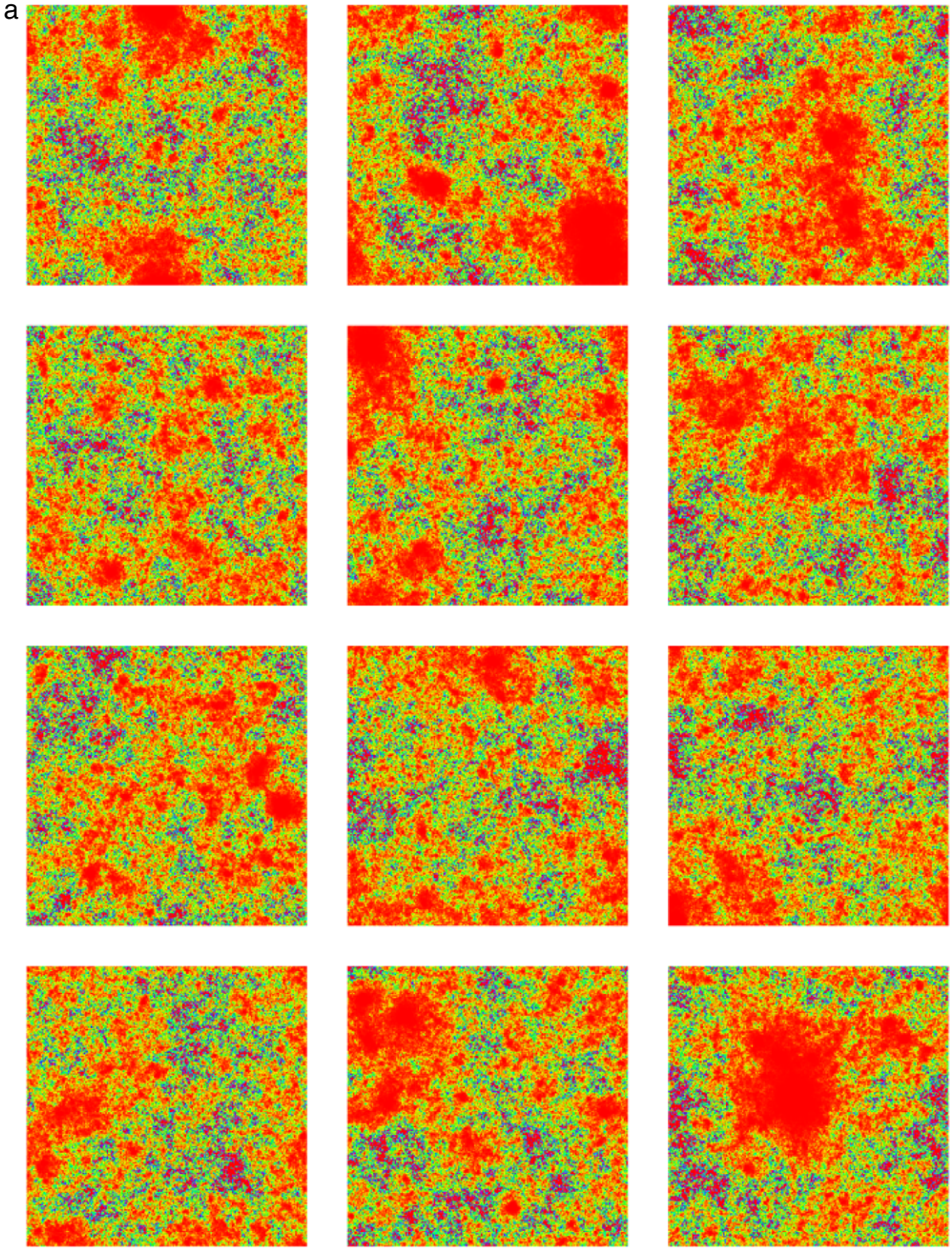

Fig. 1. (a, b) The twelve cloud density fields on 512 × 512 grids used for the Monte Carlo calculations. Above: $H = 0$. Red–orange indicates low density, purple indicates high density. Below are the same fields fractionally integrated with $H = 1/3$. (For interpretation of the references to colour in this figure legend, the reader is referred to the web version of this article.)

introduced by H. In both cases, ensemble mean of the spatially averaged density ρ is unity but the standard deviations of the realization by realization spatial means are 0.56 and 0.55 for $H = 0$, $H = 1/3$ respectively.

Please cite this article in press as: S. Lovejoy, et al., Scattering in thick multifractal clouds, Part II: Multiple scattering, Physica A (2009), doi:10.1016/j.physa.2009.05.037

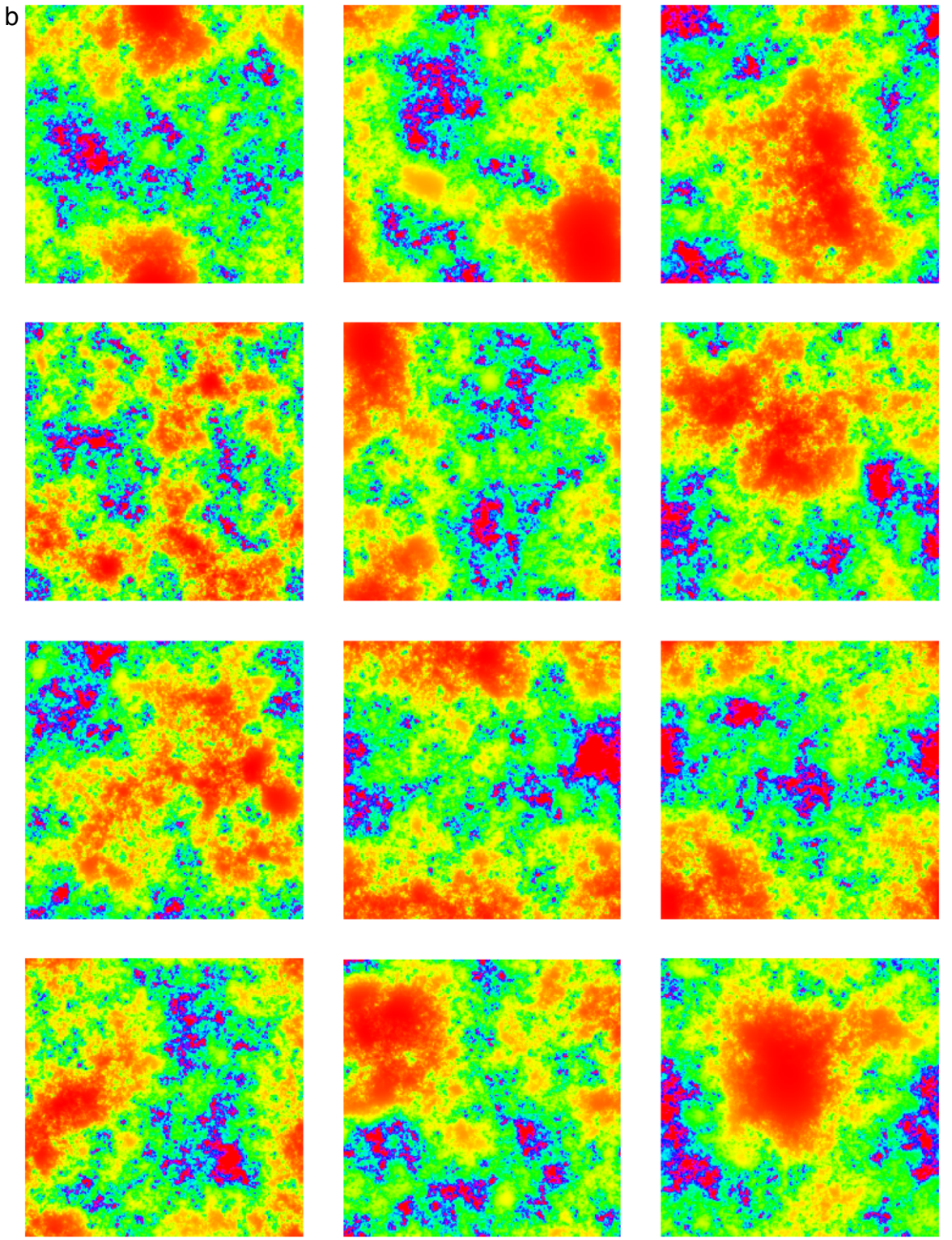

Fig. 1. (*continued*)

Before turning to Monte Carlo simulations, we can already determine the mean direct transmission of a beam pointing downward from the top of the cloud, i.e. we calculate:

Please cite this article in press as: S. Lovejoy, et al., Scattering in thick multifractal clouds, Part II: Multiple scattering, Physica A (2009), doi:10.1016/j.physa.2009.05.037

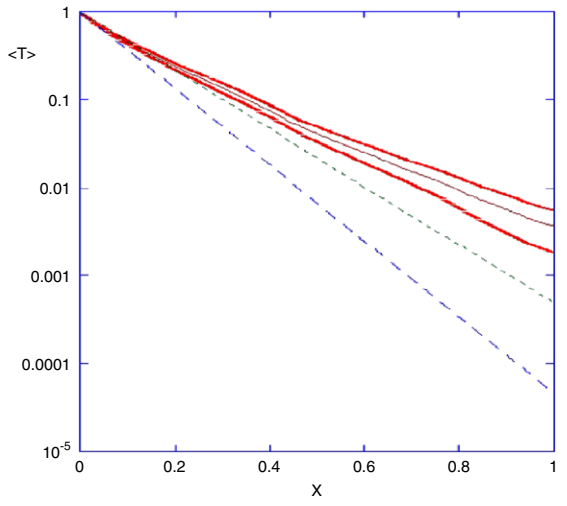

Fig. 2a. The dashed blue line (bottom) shows the profile for the multifractal cloud with $\alpha = 1.75$, $C_1 = 0.1$, $\kappa = 10$; the dashed green line (second from the bottom) indicates the result for the homogeneous cloud with renormalized $\kappa_{eff} = \kappa^{a(0)} = 7.6$, the brown (second from the top) indicates the actual mean and the red are the standard deviations.

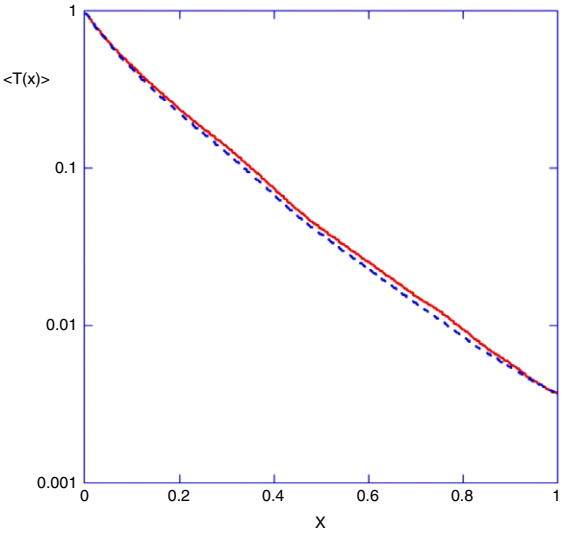

Fig. 2b. Semi-log comparison of the mean interior transmission profiles for a point source for $H = 0$ (solid line) and $H = 1/3$ (dashed line). Averages are over the 12 realizations (Fig. 1a and b), x is the fraction of the vertical height starting at the top; the transmission for the point directly below the beam, $\kappa = 10$.

$$\langle T(x)\rangle = \left\langle e^{-\kappa \int_0^x \rho(x')dx'} \right\rangle \tag{1}$$

averaging over the 12 clouds in Fig. 1a. Fig. 2a shows the mean fall-off of the radiation as the beam penetrates deeper into the cloud for $\kappa = 10$ (recall that the mean density $\langle\rho\rangle = 1$ and the thickness is 1 so that the mean optical thickness $\langle\tau\rangle = \kappa\langle\rho\rangle x = \kappa$). We see that the direct transmission is somewhat underestimated by the homogeneous and renormalized homogeneous clouds. We can also consider the non-conservative $H = 1/3$ (the Corrsin–Obukov value, close to the horizontal observations). We see that there is very little difference for the $H = 0$, $H = 1/3$ cases. To see this more clearly, Figs. 2b and 2c show that the difference between the average transmission profiles for the conservative and non-conservative clouds is less than 12% peaking near the bottom of the cloud. These results show that even in thick multifractal clouds, the degree of smoothness of the cloud (as characterized by H, but not by α or C_1 which change the transmission exponents) does not affect the transmission much.

In order to study both multiple scattering and the effect of $H > 0$, we now estimate the transfer for the clouds in Fig. 1. Probably the simplest technique is the Monte Carlo technique which is standard for radiative transfer calculations; the single scattering result was used in Part I, Section 3. To extend this to multiple scattering, photons are simulated and statistics are built up from many photons. Considering pure scattering (no absorption), after starting the photon off at a boundary

Please cite this article in press as: S. Lovejoy, et al., Scattering in thick multifractal clouds, Part II: Multiple scattering, Physica A (2009), doi:10.1016/j.physa.2009.05.037

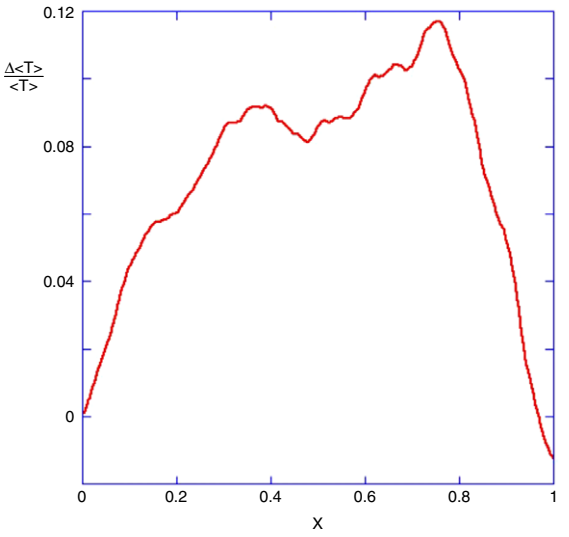

Fig. 2c. The fractional difference from the $H = 0$ case: the change is less than 12%. 256×256 grid, $\alpha = 1.75$, $C_1 = 0.1$.

in the direction of incident radiation, it propagates in a straight line until the total integrated optical thickness equals an exponential random deviate (this comes from the standard exponential propagator/Green's function, $e^{-\tau}$). The direction of the photon is then changed randomly according to the scattering phase function.

As a convenient reference process, consider first the purely homogeneous case (with isotropic discrete angle (DA) phase function i.e. the same in all of the possible orthogonal directions), for large N we can use the central limit theorem (Gaussian limit) to obtain the result:

$$\left\langle x_{N,hom}\,(\kappa)^{q_p}\right\rangle = G^{q_p}\kappa^{-q_p}N^{q_p/D_F}; \quad G = 2\Gamma\left(1+\frac{q_p}{2}\right)^{1/q_p}; \; D_F = 2 \tag{2}$$

where $x_{N,hom}$ is the distance from the starting point of a photon after N scatters, $D_F = 2$ (independent of q_p) is the fractal dimension of the photon path and G is a numerical factor which rises from 1.3 to 2 as q_p varies over the range -0.5 to 2 (the values used below). In the multifractal case we anticipate that the successive scatters never completely decorrelate; rather than obtaining a standard linear law of variance growth with number of scatters N, due to the scaling one expects an anomalous law:

$$\left\langle x_N\,(\kappa)^{q_p}\right\rangle = g\,(\kappa)\,N^{q_p/D_F(q_p)} \tag{3}$$

where x_N is the distance corresponding to $x_{N,hom}$ but for the multifractal, $D_F(q_p)$ is the "effective fractal dimension", which we anticipate will depend on q_p, (and weakly on κ; Eq. (3) is only approximately valid). In attempting to verify Eq. (2) we have a choice of either normalizing the mean spatial cloud density cloud by cloud, or alternatively only fixing the ensemble average density (e.g. only fixing the average over the independent realization shown in Fig. 1). Our use of the ensemble normalization rather than (realization by realization) normalization is not an obvious choice, but the numerics indicate that it gives more stable results, probably because the spatial average on a single realization can be sensitive to a single large singularity.

Before considering the form of the prefactor $g(\kappa)$ we can check that Eq. (3) is indeed roughly satisfied, see Figs. 3a and 3b (for $H = 0, 1/3$ respectively). We see that there is a transition from the low N, κ behavior (as predicted by Eq. (3)) to a different asymptotic scaling; Fig. 4 shows the effective fractal dimension of the asymptotic (large N) behavior. Since $D_F(q_p) > 2$, it corresponds to "subdiffusive" transport.

In order to better understand this result let us see the degree to which the renormalization idea describes the data. First, we can define the effective extinction coefficient κ_{eff} by:

$$\kappa_{eff} = \left\langle x_1^{q_p}\,(\kappa)\right\rangle^{-1/q_p}, \quad \text{valid for } q_p > -1, \tag{4}$$

where we have added the subscript "1" to indicate single scattering (i.e. $N = 1$), and we anticipate that in general κ_{eff} will be a function of both the spatial mean extinction coefficient κ and q_p. When κ is small enough, the power law is the leading term (it is always dominant for $q_p < 0$) and hence we recover $\kappa_{eff} = \kappa^{a(q_p)}$, with $a\left(q_p\right) = -\frac{\mathrm{Req}(q_p)}{q_p}$ (cf. in Part I Eq. I.45).

Now consider the homogenous (Eq. (2)) cloud, we have:

$$x_{N,hom}\,(\kappa) \approx N^{1/2}x_{1,hom}(\kappa); \quad x_{1,hom}\,(\kappa) \approx \kappa^{-1}. \tag{5}$$

We therefore have a simple relation between the statistics of N scatters in a thick cloud and single scatter statistics in a thin cloud:

$$x_{N,hom}\,(\kappa) \approx x_{1,hom}\left(N^{-1/2}\kappa\right). \tag{6}$$

Please cite this article in press as: S. Lovejoy, et al., Scattering in thick multifractal clouds, Part II: Multiple scattering, Physica A (2009), doi:10.1016/j.physa.2009.05.037

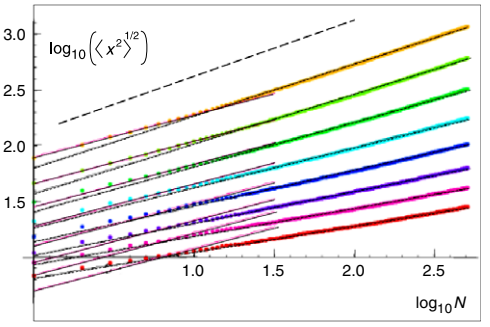

Fig. 3a. The logarithm of the $q_p = 2$ reduced moment in pixels is plotted as a function of the number of scatters. The data points are the means of 5000 walks averaged over the twelve realizations in Fig. 1a ($\lambda = 512, C_1 = 0.1, \alpha = 1.75, H = 0$). The solid dark lines are the result of Eq. I.46: $a(2)/2 = 0.38$. The dashed lines are linear fits to the large N portions. κ increases from top to bottom (32, 64, ..., 4096). The coarsely dashed reference line of slope $\frac{1}{2}$ shows the standard homogeneous diffusion result.

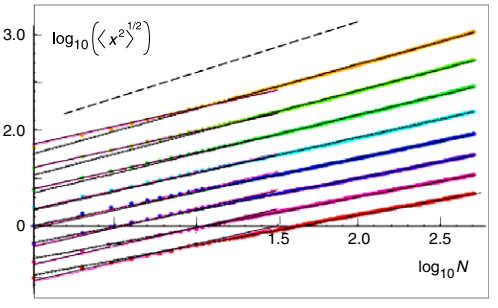

Fig. 3b. The same as in Fig. 3a except from analysis of Fig. 1b, i.e., with $H = \frac{1}{3}$. Note the similarity.

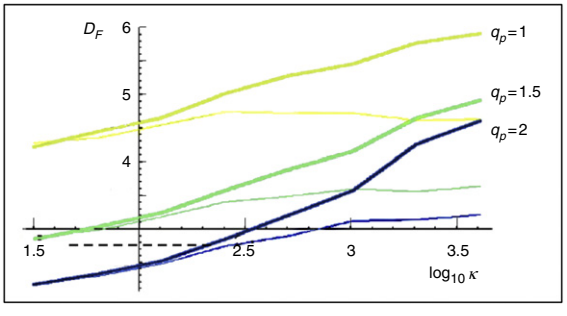

Fig. 4. The effective fractal dimension as a function of κ for various moments of the photon path length q_p ($H = 0$, thick line, $H = 1/3$, thin line). These values are estimated from regressions on Figs. 3a and 3b for N in the range 128 to 512. $D_F > 2$ indicates subdiffusion. For comparison, the short dashed line shows the single scattering prediction: $D_F(q_p) = 2/a(q_p)$ implies $D_F(2) = 2.60$. with $D_F(1.5)$, $D_F(1)$ slightly smaller (2.53, 2.45 respectively).

If the cloud can be "renormalized" we therefore suppose that a similar relation exists in the multifractal cloud:

$$x_N(\kappa) \approx x_1\left(N^{-1/2}\kappa\right) \tag{7}$$

where x_1, x_N are for the multifractal single and Nth multiple scattering distances respectively. In terms of moments:

$$\left\langle x_N^{q_p}(\kappa)\right\rangle \approx \left\langle x_1^{q_p}\left(N^{-1/2}\kappa\right)\right\rangle \tag{8}$$

i.e. we assume that the only difference is that the multifractal function $x_1(\kappa)$ is quite different from the homogeneous $x_{1,hom}(\kappa)$; indeed from Eq. I.39, 40, we have $\left\langle x_1^{q_p}(\kappa)\right\rangle$ expressed in terms of an integral, or in terms of a series, Eq. I.43. We used it (c.f. Eq. I.47) to define the effective κ (Eq. (4)), which, when combined with Eq. (8), we thus predict that:

$$\frac{\left\langle x_N(\kappa)^{q_p}\right\rangle^{1/q_p}}{\left\langle x_1\left(N^{-1/2}\kappa\right)^{q_p}\right\rangle^{1/q_p}} = \kappa_{eff}\left(N^{-1/2}\kappa\right)\left\langle x_N(\kappa)^{q_p}\right\rangle^{1/q_p} \approx \text{constant} \tag{9}$$

Please cite this article in press as: S. Lovejoy, et al., Scattering in thick multifractal clouds, Part II: Multiple scattering, Physica A (2009), doi:10.1016/j.physa.2009.05.037

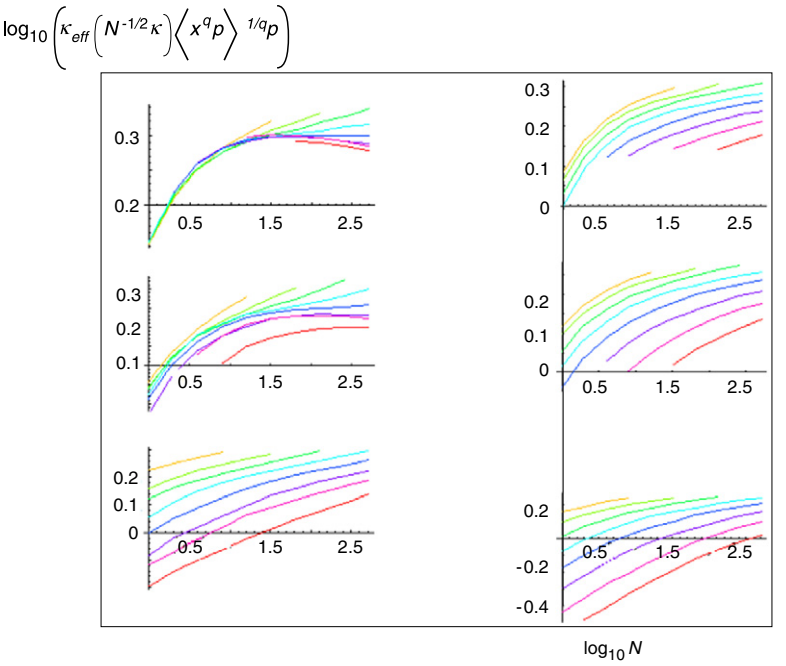

Fig. 5. The Monte Carlo reduced photon path moments for N scatterings in clouds (depicted in Fig. 1) of varying mean thickness $\langle\kappa\rangle$ "compensated" using the theoretical single scattering formula but with thickness $N^{-1/2}\langle\kappa\rangle$; the abscissa is $\left\langle x_N(\kappa)^{q_p}\right\rangle^{1/q_p} / \left\langle x_1\left(N^{-1/2}\kappa\right)^{q_p}\right\rangle^{1/q_p}$, c.f. Eq. (9). Each graph displays $\kappa = 32, 64, \ldots, 4096$ top to bottom. Each column shows the moments $q_p = -0.5, 1.0, 2.0$ top to bottom, with $H = 0$ on the left and $H = 1/3$ on the right. Perfect compensation would give horizontal lines at zero. Homogeneous clouds (with κ_{eff} replaced by κ) would give horizontal lines at $\log_{10} G$ (see Eq. (2)) rising from 0.13 ($q_p = -0.5$) to 0.3 ($q_p = 2$).

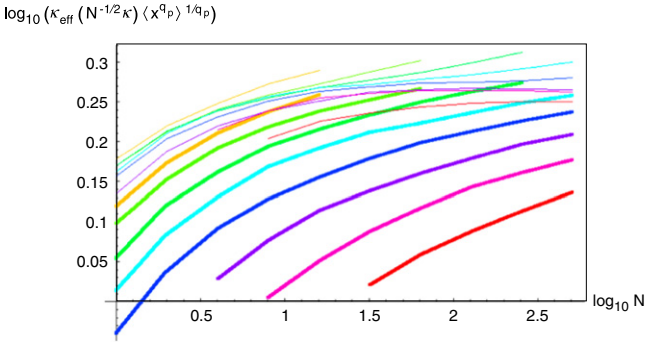

Fig. 6a. The compensated $q_p = 1$ reduced moments, $H = 0$ (thin), $H = 1/3$ (thick) from Fig. 5. Curves top to bottom are for $\kappa = 32, 64, \ldots, 4096$.

and using $\kappa_{eff}(\kappa) \approx \kappa^{a(q_p)}$ (Eq. I.47) we obtain:

$$\left\langle x_N^{q_p}(\kappa)\right\rangle \approx \left(N^{-1/2}\kappa\right)^{-a(q_p)q_p} = \kappa^{-a(q_p)q_p} N^{a(q_p)q_p/2}. \tag{10}$$

This predicts that the fractal dimension of the walk is $D_F = 2/a(q_p)$, $g(\kappa) \approx \kappa^{-a(q_p)q_p}$. We use the twelve multifractal simulations shown in Fig. 1a to test this. The Monte Carlo numerics are used to estimate the N scatter statistics (the numerator in Eq. (9)) whereas the exact single scattering theory is used in the denominator (using the numerical integral Eq. I.40 to determine W in Eq. I.42). In Figs. 3a and 5 we see that this prediction is indeed verified for small enough N and κ; however we also see that the asymptotic exponent is somewhat different; Fig. 4 shows that $D_F(q_p)$ increases with κ.

For a given q_p we see that Eq. (8) is indeed valid to within a factor of about 2, and this with κ varying between 32 and 4096 and N from 1 to 512, an impressive agreement. Note that to ensure reasonably reliable random walk averages, in Fig. 5a only those values of $\left\langle x_1^{q_p}(\kappa)\right\rangle^{1/q_p}$ in the range of 3 to 200 pixels on the simulations were used since below one pixel, the simulation is too smooth and above 512 pixels it is periodic and therefore no longer scaling.

We can now consider the effect of fractional integration using $H = 1/3$ (the Corrsin–Obukov value, close to atmospheric observations in the horizontal, see the realizations in Fig. 1b). In Figs. 3b and 5 we see that the fractional integration changes

Please cite this article in press as: S. Lovejoy, et al., Scattering in thick multifractal clouds, Part II: Multiple scattering, Physica A (2009), doi:10.1016/j.physa.2009.05.037

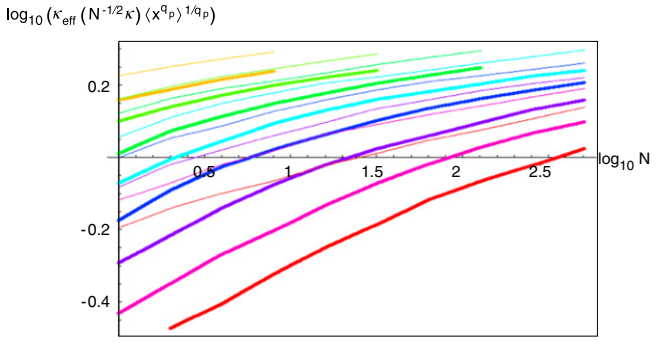

Fig. 6b. The compensated $q_p = 2$ reduced moments, $H = 0$ (thin), $H = 1/3$ (thick) from Fig. 5. $H = 0$ (thin), $H = 1/3$ (thick). Curves top to bottom are for $\kappa = 32, 64, \ldots, 4096$.

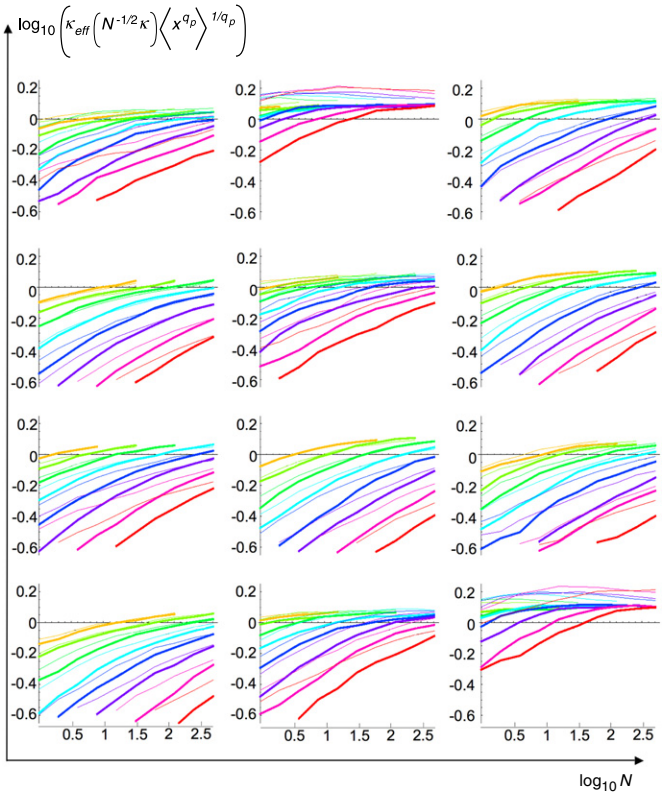

Fig. 7. This shows the cloud to cloud variability; each graph corresponding to one of the 12 clouds shown in Fig. 1. This shows the multiple scatter predictions of Eq. (8) where the spatial mean of κ is used instead of the ensemble mean. Each graph corresponds to the $H = 0$ and $H = 1/3$ simulations shown in Fig. 1a and b respectively (for $q_p = 2$). Each color corresponds to a different κ; the latter increasing from top to bottom from 32 to 4096 in steps of factors of 2. For a given κ, the $H = 0$ curve is always above the corresponding $H = 1/3$ curve.

the multiple scattering statistics surprisingly little; this is quantified for the exponents (the fractal dimensions of the walks, Fig. 4). We see that there is virtually no difference for $\kappa \leq 100$. For very large κ, $D_F(\kappa, H = 0) > D_F(\kappa, H = 1/3)$ so that the effect of fractional integration on the walk is to make the latter less clustered.

It is perhaps somewhat surprising that the effect of the fractional integration order $H = 1/3$ is so small. To make the comparison easier, we display the plots for both H values on a single plot in Figs. 6a and 6b for $q_p = 1, 2$. We see that Eq. (9) (and hence Eq. (7)) works somewhat better for $H = 0$ than for $H = 1/3$, but the latter is still valid to within a factor of about 4 over the entire range of N, κ.

In applications, the radiance fields can be considered to be a superposition of fields, one for each order of scattering. Although we consider the case of "plane parallel" boundary conditions in the next sections, we can already remark that the tendency for D_F to increase with increasing κ (Fig. 4) and for the ratio $\langle x_N(\kappa)^{q_p}\rangle^{1/q_p} / \langle x_1(N^{-1/2}\kappa)^{q_p}\rangle^{1/q_p}$ to systematically decrease with increasing κ to indicate that thick clouds will transmit *less* than that predicted by simple renormalization using $\kappa_{eff} = \kappa^{a(q_p)}$. This is directly confirmed in the next section. Thus, while the thick cloud single scatter transmission is

Please cite this article in press as: S. Lovejoy, et al., Scattering in thick multifractal clouds, Part II: Multiple scattering, Physica A (2009), doi:10.1016/j.physa.2009.05.037

greater than that predicted by renormalization (the log terms in Eq. I.46), this effect is somewhat countered by increasing clustering of the photon path statistics.

Finally, we can consider the cloud to cloud variability. Fig. 7 shows the cloud by cloud results (from the density fields of Fig. 1) for $q_p = 2$ when Eq. (8) is used with the spatial mean of the specific realization instead of the ensemble mean. We see that the cloud to cloud variability is not so large.

2. The DART phase functions and multiple scattered radiation

For estimating the radiance fields in optically thick media, Monte Carlo methods are very noisy. One way to improve on this is the "stochastic radiative transfer" method proposed by Evans [7] which could be regarded as a generalization of the single scattering method developed in Section 3 to double, triple, N scatters. However, these extensions require knowledge of all the joint probabilities of the multiple scatter distances so that the method is only practical when scattering is of low order or when correlations between successive scatters are weak (an assumption not valid in thick multifractal clouds). Instead we will attempt to directly numerically solve the radiative transfer equation. To date, many numerical and theoretical approximation methods have been developed to handle transfer in heterogeneous media with arbitrary phase functions (e.g. the Spherical Harmonics Discrete Ordinate method [8]; for a review of numerical methods see Gabriel et al. [9] and Lane-Vernon et al. [10] for binary Markovian cloud models). Unfortunately, the extreme variability of realistic cloud models (whether multifractal or from numerical fluid dynamical simulations) is such that most of these numerical radiation schemes are pushed to their limits. The result is that there has developed a huge effort just to intercompare the different transfer numerical schemes (c.f. the C^3 initiative [11]). In order to progress, it is imperative to have quick and reliable transfer calculations so that the technical details of the transfer calculation do not stand in the way of our understanding of the effects of cloud variability. One way to achieve this is by using special discrete angle phase functions (DA radiative transfer [12]), so that in 2D, the radiative fields are only coupled in 4 orthogonal directions, it nevertheless allows the effects of cloud inhomogeneity to be studied in detail. It is important to emphasize that we do not consider the special DA phase functions as approximations to more general ones, rather we seek to understand the effect of extreme multifractal spatial variability on the associated radiation fields. As shown in Lovejoy et al. [12], the thick cloud DA scaling exponents do not depend on the scattering phase function so that the special choice of phase function should not be important for our understanding of multifractal heterogeneity. As we indicate below, it has the advantage of making the numerics more exact and rapid.

In 2-D DART, the radiative transfer equation can be expressed in a four-stream scattering function inducing a similar decomposition of the radiance field [12]:

$$\left[A_x \frac{\partial}{\partial x} + A_z \frac{\partial}{\partial z}\right] \mathbf{I}\left(\underline{x}\right) = \kappa \rho \left(\underline{x}\right) \left(\mathbf{P} - \mathbf{1}\right) \mathbf{I}\left(\underline{x}\right) \tag{11}$$

where $\mathbf{1}$ is the 4×4 identity matrix, κ the extinction coefficient, ρ the cloud liquid water density and:

$$A_x = \begin{pmatrix} 1 & 0 & 0 & 0 \\ 0 & -1 & 0 & 0 \\ 0 & 0 & 0 & 0 \\ 0 & 0 & 0 & 0 \end{pmatrix}; \qquad A_z = \begin{pmatrix} 0 & 0 & 0 & 0 \\ 0 & 0 & 0 & 0 \\ 0 & 0 & 1 & 0 \\ 0 & 0 & 0 & -1 \end{pmatrix} \tag{12}$$

$$\mathbf{I} = \begin{pmatrix} I_{+x} \\ I_{-x} \\ I_{+z} \\ I_{-z} \end{pmatrix}; \qquad \mathbf{P} = \begin{pmatrix} t & r & s & s \\ r & t & s & s \\ s & s & t & r \\ s & s & r & t \end{pmatrix}$$

the $\mathbf{I}$ vector represents the intensities in the four orthogonal directions $+x, -x, +z, -z$ respectively, the matrix $\mathbf{P}$ is the DART phase function with coefficients t, r, s for transmission, reflection and side scattering respectively. The "single scattering albedo" is $\omega_0 = r + t + 2s$; for conservative scattering $\omega_0 = 1$. Also, the standard phase function "asymmetry factor" is $g = (t - r)\omega_0$ [12]. This system can be viewed as a direct descendent of the original two-stream theory in 1-D.

The following finite difference system [12]

$$I_i\left(\underline{m}l\right) = \sum_{j=1}^{4} \sigma_{i,j}\left(\underline{m}l\right) I_j\left(\left(\underline{m} - \underline{k}(j)\right) l\right) \tag{13}$$

$$\sigma = \begin{pmatrix} T & R & S & S \\ R & T & S & S \\ S & S & T & R \\ S & S & R & T \end{pmatrix}$$

can be used to approximate the 2D DA system; $\underline{m}$ is an integer valued position vector, l the lattice spacing, and the sum is over $\underline{k}(j) = (1, 0), (-1, 0), (0, 1), (0, -1)$ for $j = 1, 2, 3, 4$ respectively. For a lattice cell with optical thickness τ_0, the relation between finite difference matrix σ and the PDE $\mathbf{P}$ matrix is:

$$\sigma = \left(\mathbf{1} + \left(\mathbf{1} - \mathbf{P}\right) \tau_0\right)^{-1}. \tag{14}$$

Please cite this article in press as: S. Lovejoy, et al., Scattering in thick multifractal clouds, Part II: Multiple scattering, Physica A (2009), doi:10.1016/j.physa.2009.05.037

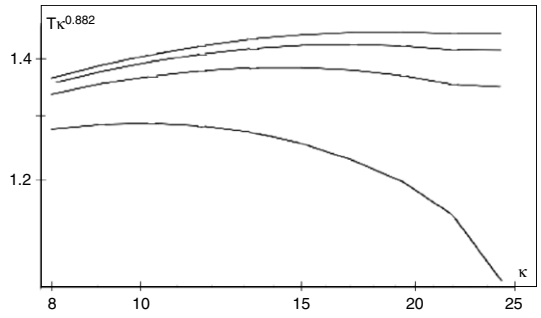

Fig. 8a. Mean transmission compensated by the theoretical power law behavior ($T\kappa^{a(0)}$ versus log κ scale; $a(0) = \left(1 + \frac{C_1}{\alpha - 1}\right)^{-1} = 0.882, \alpha = 1.75$, $C_1 = 0.1, H = 0$) for a single multifractal cloud ($8 \leq \kappa \leq 25$) developed over a range of scales of factor 50, periodic boundary conditions on the sides. The resulting field was then discretized over 50×50, 100×100, 150×150 and 200×200 pixel grids (bottom to top respectively) and Eq. (13) solved. As the resolution increases, the error decreases; the compensated transmission appears to converge. As expected, we notice a small discrepancy with respect to the theoretical transmission curve at small κ (the latter is only an asymptotic approximation). At large κ, for large enough λ, $\kappa^{0.882}T$ is flat as expected.

When τ_0 is small enough, the solution of the finite difference scheme Eq. (13) converges to the solution of the PDE in Eq. (11).

The calculations below are in 2-D using 4 orthogonal angles. Although radiation fields may exist in arbitrary directions, they are only coupled in these four directions which can be chosen parallel with standard Cartesian axes used for the spatial discretization of the transfer equations. The latter are then reduced from a partial integro-differential equation to sets of four coupled partial differential equations for each quadruplet of orthogonal directions. The result is that the only significant source of numerical error is in the spatial discretization (i.e., the use of Eq. (13) instead of Eq. (11)). Finally, the actual numerical solution of Eq. (13) can benefit by the advances being made in the last ten years in sparse matrix numerics. In what follows, we can solve 512×512 systems to 16 figure precision in less than a minute on a Macintosh computer effectively inverting a sparse 2^{20} by 2^{20} element matrix, gaining enormously over earlier relaxation methods (see, e.g., Ref. [13]). It is worth noting [12] that in optically thick multifractal clouds the expected scaling exponents (e.g., the mean transmission as a function of the total optical depth) do not depend on the phase functions (the prefactors however do depend on them), hence DART allows us to determine the general scaling properties of the radiation fields.

In order to validate the numerics and to study the effect of the discretization of the DA PDEs, we show numerical simulations of radiative transfer in multifractal clouds with $\omega_0 = 1$ (i.e., no absorption for conservative scattering), and with a DA isotropic phase function (the four orthogonal directions of scattering angle have equal probabilities of occurrence, i.e., $s = r = t = 1/4$; the asymmetry factor is therefore $g = 0$). Note that exact DA similarity relations exist [12], so that with these solutions one may obtain exact solutions (at least for boundary conditions with simple symmetries) of the transfer for any DA phase function from solutions of any other DA phase function. Although the choice of an isotropic phase function is somewhat arbitrary, it was made due to its relatively rapid approach to the thick cloud limit (although the optimum in this regard are the phase function parameters $s = 1/2, r = t = 0$).

The use of conservative scattering ($\omega_0 = 1$) is a good choice for terrestrial clouds at wavelengths where absorption can be neglected. Indeed, at visible wavelengths clouds are characterized by $\omega_0 > 0.99$ so that even in moderately thick clouds many orders of scattering actually contribute to the total radiation field. We therefore used DA phase functions and "plane parallel" type boundary conditions i.e. uniform incident overhead intensity = 1 at the cloud top, and with cyclic boundary conditions on the left and right sides. The incident flux is monodirectional and monochromatic and we neglected any internal sources of radiation (such as those due to thermal emission, important at thermal IR wavelengths). These choices can be considered as the "plane parallel" analogs for multifractal clouds.

For comparison purposes, recall the exact solution for a sourceless homogeneous atmosphere, and pure scattering. Since $\langle \rho \rangle = 1, L = 1$ (the cloud size) and $\langle \tau \rangle = \kappa \langle \rho \rangle L = \kappa$ so that κ is the mean optical thickness, the albedo of the entire homogeneous slab is given by $R = \frac{\tilde{\kappa}}{2+\tilde{\kappa}}$, with the similarity relation $\tilde{\kappa} = (1-g)\kappa$, and the transmittance is:

$$T = 1 - R = \frac{2}{2 + \tilde{\kappa}}. \tag{15}$$

For typical cloud droplet distributions and for visible wavelengths g is generally chosen constant with values in the range 0.80–0.85. In our simulations below, we chose $g = 0$ which implies the trivial equality $\tilde{\kappa} = \kappa$. For large enough κ, the transmission in a homogeneous cloud (or equivalently, with the chosen boundary conditions, in a plane parallel cloud) therefore simply scales as $T \propto \kappa^{-1}$.

3. Radiance fields for isotropic multifractal clouds with "plane parallel" boundary conditions

Since multifractals are highly variable, in practice, some truncation of high κ, ρ values is inevitable. Since the optically thick pixels transmit little radiation, this truncation of a small fraction of the pixels need not be too significant. In Figs. 8a and 8b, we show the effect of systematically improving the spatial resolution on an isotropic multifractal cloud. All pixels

Please cite this article in press as: S. Lovejoy, et al., Scattering in thick multifractal clouds, Part II: Multiple scattering, Physica A (2009), doi:10.1016/j.physa.2009.05.037

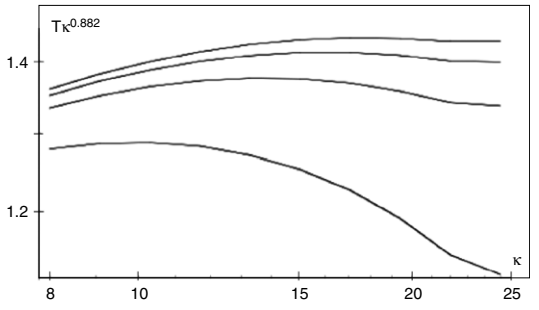

Fig. 8b. The same as Fig. 8a but with $H = 1/3$.

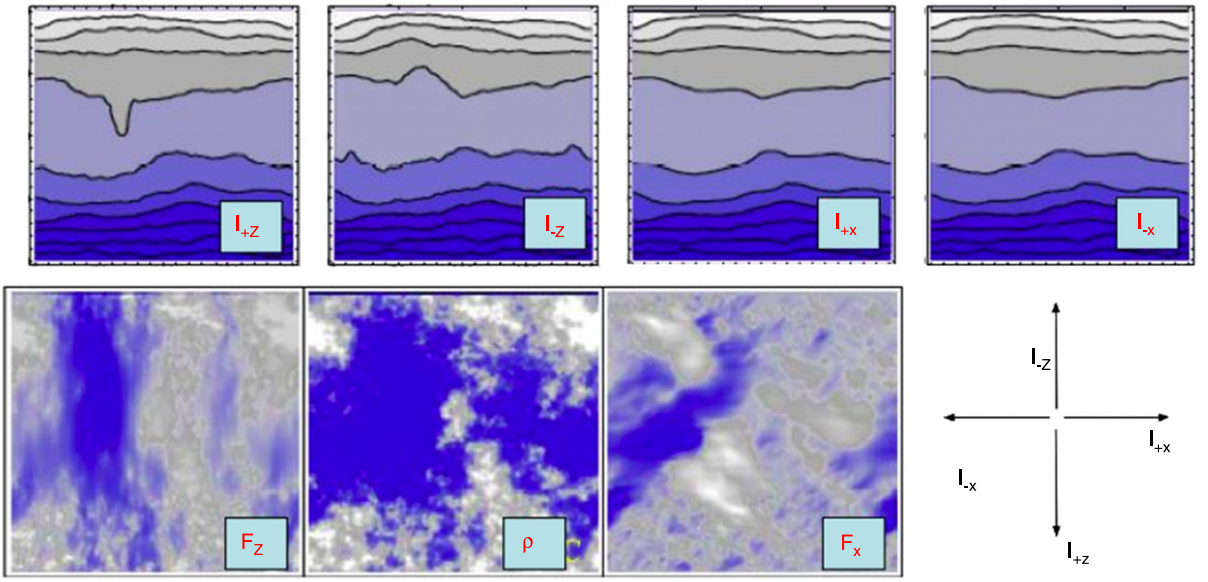

Fig. 9a. This shows the results of DA radiative transfer calculation on a multifractal cloud (density, middle bottom row, $\alpha = 1.75, C_1 = 0.1, H = 0$), with spatial mean optical thickness 100, the simulations are on a 200×200 grid and the incident radiation is from the top (isotropic DA phase functions). Top shows radiances, bottom far left vertical flux, far right, horizontal flux.

that had an optical thickness greater than 0.5 at the highest κ used (here $= 25$), were truncated to 0.5. Fig. 8 shows that for multifractal clouds, the main effect of inadequate resolution is (as expected) for the extreme optically thick clouds where it artificially decreases the transmission. The asymptotic flatness of the large λ graph of the theoretically compensated mean transmittance is strong evidence that the single scattering theory which predicts an "effective $\kappa = \kappa^{a(0)}$ works reasonably well for multiple scattered radiation (λ is the number of pixels on each side).

To get an idea of the various radiation fields, Figs. 9a and 9b show simulations of a multifractal cloud and associated radiance fields for $\kappa = 100$, on a 200×200 point grid with $H = 0, 1/3$ respectively. The incident radiation is in the I_{+z} direction (down in the figure), and the boundary conditions are periodic in the left-right ($\pm x$ directions). We note that there is not a strong difference between the $H = 0$ and $H = 1/3$ radiances and that the different radiance fields seem all qualitatively quite similar; it is more revealing to study the horizontal and vertical fluxes (F_x, F_z), the latter are the difference of radiances: $F_i = I_{+i} - I_{-i}$ for $I = x, z$ (for conservative scattering as here, the divergence of $\underline{F}$ is zero). The fluxes are relatively easy to correlate with the cloud density field; it is clear that most of the down flux is (as expected) in the low cloud density region; but that the detailed flux distributions are nontrivially related to the cloud density.

In order to see more clearly the relation between the fluxes, cloud density and extinction coefficient, we refer the reader to Fig. 10 which shows the flux lines (i.e. the lines whose tangent is everywhere parallel the the flux vector $\underline{F}$). One can see the tendency for the flux lines to be "attracted" to regions of low optical density and "repelled" by regions of high optical density. This tendency for radiative "channeling" [14] is more and more pronounced as κ increases. Since the scattering is conservative, radiant energy which starts off at the top between two flux lines remains between the flux lines (note that this is *not* the same as saying that the simulated photons stay trapped between the flux lines).

In order to quantify the overall effect of the multifractality on the mean cloud transmittance for various α, H values and for increasing optical thicknesses, we refer the reader to Fig. 11. This figure shows both the mean and spread using 10 multifractal simulations and compares the results to the theoretical prediction using homogeneous scattering renormalized

Please cite this article in press as: S. Lovejoy, et al., Scattering in thick multifractal clouds, Part II: Multiple scattering, Physica A (2009), doi:10.1016/j.physa.2009.05.037

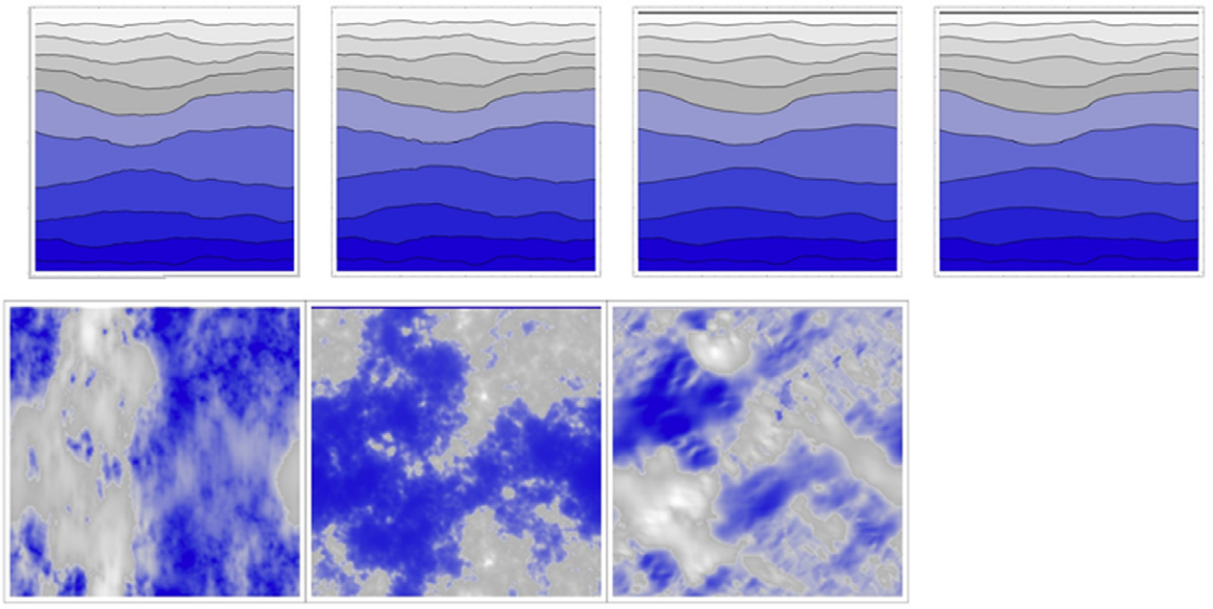

Fig. 9b. Same as Fig. 9a (including same starting "seed" so that the cloud field (bottom, middle) is only a little smoother), but for $H = 1/3$. Note that the fields are somewhat smoother than the corresponding $H = 0$ fields, but that the difference is small.

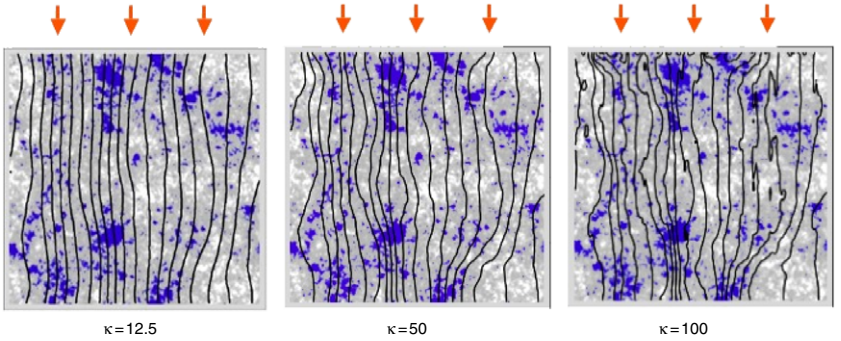

Fig. 10. For simulations with $\alpha = 1.75, C_1 = 0.1, H = 0$ and for κ increasing from left to right, radiation incident at the top, periodic boundary conditions, we show representative flux lines, the false colors indicate the relative optical density. Calculations were performed on a 200×200 pixel grid.

$\kappa_{eff} = \kappa^{a(0)}$. We see that the theoretical predictions are quite well respected although there is a slight tendency for the transmittance at the largest κ to be a bit too small. Recall that although the asymptotic theoretical result for single scattering predicts large κ deviations in the other direction (the log κ corrections in Eq. I.43, the effect of the low κ "holes" on single scattering). However, the results in Fig. 11 have much multiple scattering and in Section 1 we showed that the fractal dimension of the walks tends to increase, implying that long distance transmission decreases with respect to the renormalized single scattering prediction; the photons tend to get "stuck" in optically dense regions. The downward curvature in Fig. 11 is thus probably a real consequence of the latter rather than a numerical artefact (although for $\kappa = 100$, the simulations are near their extreme large κ limit). From Fig. 11 we can obtain a rough quantification of the deviation of the power law renormalized can be found by shifting the yellow lines up so that they fit the small κ part of the curve and the deviations can be determined at $\kappa = 100$. For $\alpha = 1.5$, we find deviations of 9%, 40%, 50% for $H = 0, 0.33, 0.66$ respectively. The corresponding numbers for $\alpha = 1.75$ are 4%, 7%, 32%.

4. Non-conservative "plane parallel" multifractal clouds

We have seen in Section 1 that the multiple scattering statistics are surprisingly little affected by a fractional integration of order H. In Section 3 we gave some numerical results on the numerical solutions of the DA radiative transfer equations investigating the overall radiance fields and hence radiative fluxes also finding that the effect of varying H was relatively small. This issue is important since realistic terrestrial clouds have (horizontal) H near the Corrsin–Obukov value 1/3.

It is of interest to directly compare the effect of multifractality on the transmissions with respect to the corresponding plane parallel cloud. If we try to estimate the cloud thickness using the observed radiances (as for example one might do

Please cite this article in press as: S. Lovejoy, et al., Scattering in thick multifractal clouds, Part II: Multiple scattering, Physica A (2009), doi:10.1016/j.physa.2009.05.037

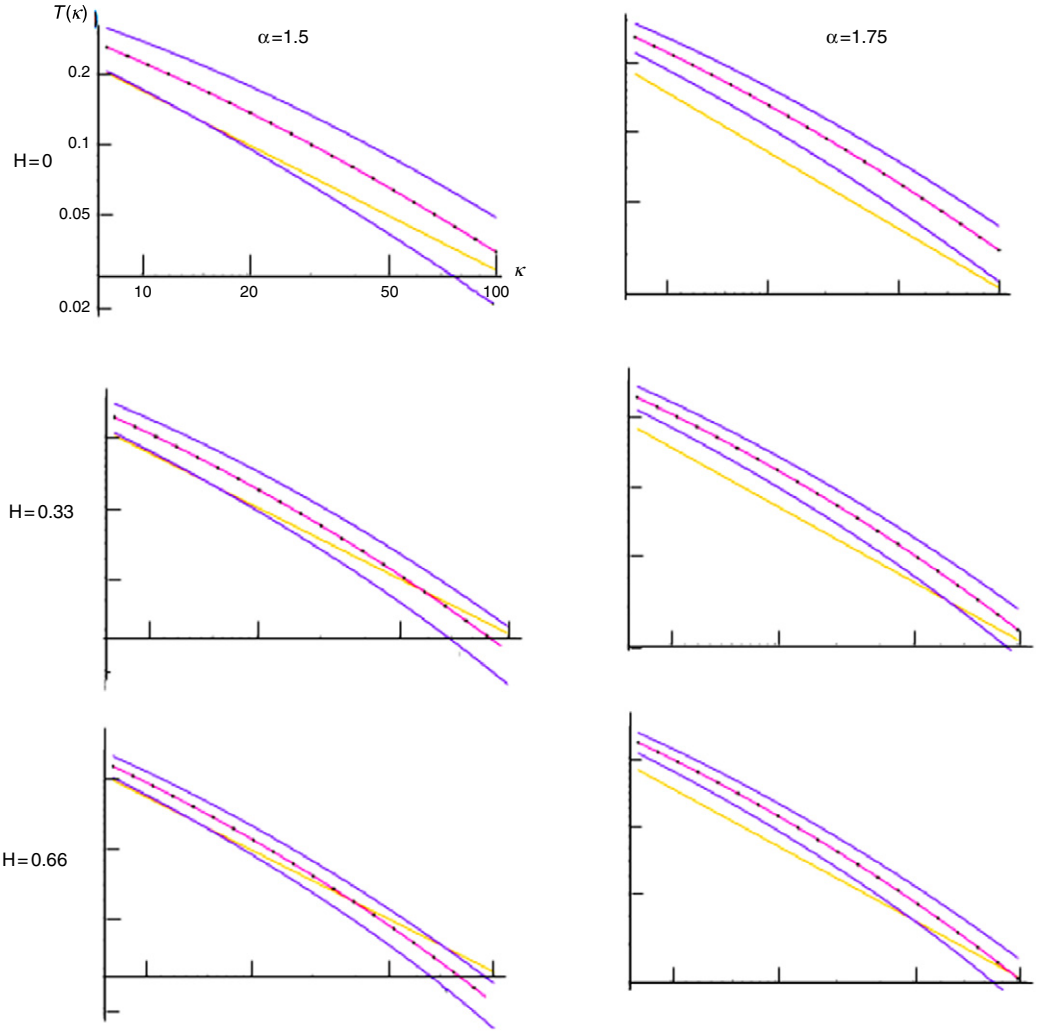

Fig. 11. The transmissions versus κ from DART simulations (isotropic phase functions). Orange (straight) reference lines are the renormalized exponent ($a(0) = 0.882, 0.833$ for $\alpha = 1.75, 1.5$ respectively), the red lines (through the points) are the means, the blue lines (upper and lower curved lines) show one standard deviation spreads (which is due to cloud to cloud variability, not error). For each plot, there were 10 simulations were on 200×200 grids. Note the small effect of increasing H and the accuracy of the power law renormalization approximation up to $\kappa \approx 50$.

from satellite imagery), then the bias is not in the transmission for a given cloud thickness, but rather in the cloud thickness for a given transmission (reflectance). For example, using the plane parallel formula (Eq. (15)), the numerics allow us to estimate an effective "plane parallel" renormalized extinction coefficient $\kappa_{eff,par}$ via:

$$\kappa_{eff,\mathrm{par}} = 2\left(\frac{1}{\langle T\rangle} - 1\right) = \frac{\kappa}{\zeta} + 2\left(\frac{1}{\zeta} - 1\right); \quad \zeta = \frac{\langle T(\kappa)\rangle}{T_{hom}(\kappa)} = \langle T(\kappa)\rangle\left(\frac{\kappa+2}{2}\right). \tag{16}$$

With the above numerics, we see that for $\kappa = 100$, with the bias is $\zeta \approx 0.75 \pm 0.15$ so that $\kappa_{eff,par} \approx 75 \pm 15$ We also see that $\kappa_{eff,\mathrm{par}} \approx \kappa/\zeta$ so that the bias in the optical thickness when estimated using plane parallel assumptions is approximately the reciprocal of the bias in the mean transmittance; for $\kappa = 100$ this is $1/\zeta \approx 1.35 \pm 0.25$. Note the wide cloud to cloud dispersion (not error) in the biased values.

In Fig. 12a, the red curve shows the ratio of the mean transmission within a multifractal cloud over the transmission within a homogeneous cloud as a function of κ for $H = 1/3$, $\alpha = 1.75$ and $C_1 = 0.1$. The black curves show this ratio plus or minus one standard deviation: again, *the spread is due to variability, not error*. As expected, we see that photons can much more easily cross the multifractal inhomogeneous cloud, in particular at large κ. For clouds with a total optical thickness of 100 this is a non-negligible ≈35% effect with respect to homogeneity. In addition, the cloud to cloud variability will be high; roughly another ±20%–25% about the (biased) mean. In Fig. 12b, we show the systematic variation of the mean transmittance as a function of κ for increasing values of H. We see that even at $\kappa = 100$, as H increase from 0 to 0.45, the mean transmission increases only about 10% so that the $H = 0$ results work fairly well.

Please cite this article in press as: S. Lovejoy, et al., Scattering in thick multifractal clouds, Part II: Multiple scattering, Physica A (2009), doi:10.1016/j.physa.2009.05.037

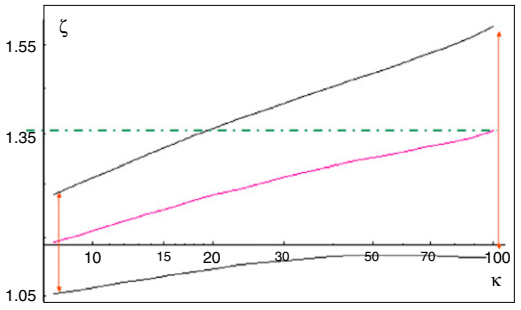

Fig. 12a. The ratio of mean (red) multifractal to homogeneous transmission as a function of mean optical thickness κ with bounding black lines show the realization to realization variability (40 realizations were used). $H = 1/3$, $\alpha = 1.75$, and $C_1 = 0.1$, using isotropic DA phase functions. (For interpretation of the references to colour in this figure legend, the reader is referred to the web version of this article.)

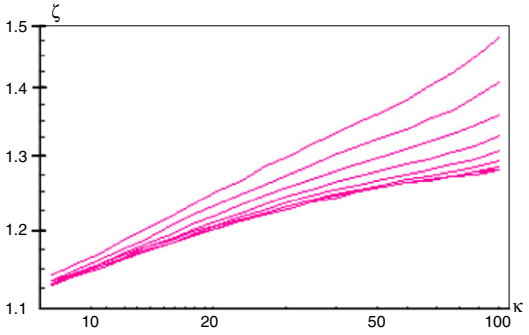

Fig. 12b. This shows ζ, the ratio of mean transmittance through multifractal clouds divided by the transmittance through the corresponding homogenous cloud for increasing mean κ for multifractal clouds with $\alpha = 1.75$, $C_1 = 0.1$. The lines from top to bottom are for $H = 0.1$ to $H = 0.9$ in increments of 0.1 (the curves for $H = 0.6$ to 0.9 are virtually indistinguishable). The realization to realization spreads (not shown) are large, comparable to those shown in Fig. 12a which shows the special case $H = 1/3$.

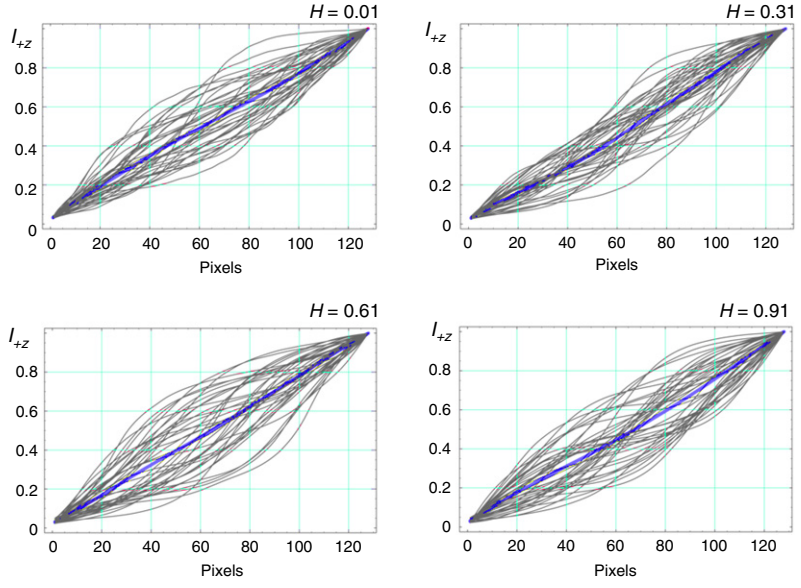

Fig. 13. The horizontally averaged downward internal radiance as a function of height (the incident radiance is at 128 pixels, exiting the cloud at 0). The line shows the average of 40 realizations at $\kappa = 64$.

5. The effect of changing *H* on the Internal radiance fields

In the previous subsections, we have considered mostly the overall mean ("bulk") transmission through a multifractal cloud. Although a study of the statistics of the variability of the transmission field (not just the spatial mean) is an important

Please cite this article in press as: S. Lovejoy, et al., Scattering in thick multifractal clouds, Part II: Multiple scattering, Physica A (2009), doi:10.1016/j.physa.2009.05.037

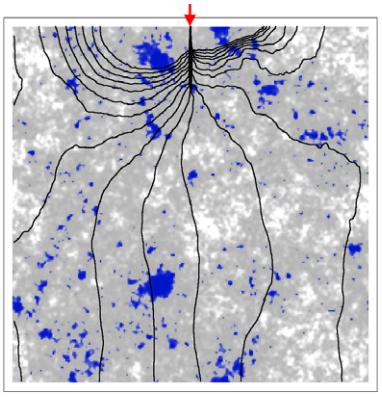

Fig. 14a. The density of multifractal cloud on a 256 × 256 grid shown as false colors with flux lines superposed, downwards point source radiation is incident as indicated by the red arrow ($\alpha = 1.75$, $C_1 = 0.1$, mean $\kappa = 50$, isotropic DA phase functions). (Compare to the middle plot of Fig. 10, which is the same except for using uniform sources).

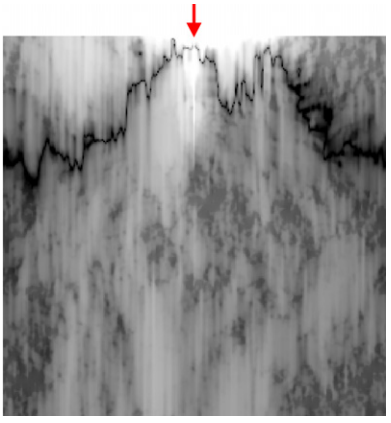

Fig. 14b. The gray scale shows the log of the absolute vertical flux for the point source indicated.

future task, it is of interest to take a quick look at the internal variability of the multifractal clouds. In these examples, we used 128 × 128 fields having $\alpha = 1.75$ and $C_1 = 0.1$ for various values of H and with $\kappa = 64$. In Fig. 13, we show from 40 realizations the profiles of the horizontally averaged downward intensity I_{+z} (vertical intensity going downward) and the mean intensity profile (pink). Whatever the value of the total maximum κ or the value of H, we see that the mean converges towards a near straight line, (as for scattering within a homogeneous medium). However near the middle of the cloud, the mean varies between 0.2 and 0.8 which is very large indeed. On the other hand, the near linearity of the ensemble mean suggests that this could be a useful statistical closure type approximation, a possibility that we do not pursue here.

6. Non-conservative point source multifractal clouds

In Sections 2–5 we used boundary conditions with incident radiation along the top of the cloud. It is also of interest to study the radiation fields associated with simpler boundary conditions such as a single point source at the cloud top, corresponding for example to a downward pointing laser beam. Although the mean direct transmittance for this case was discussed in Section 1 (Figs. 2a–2c), we now revisit this effectively considering all orders of scattering using DART numerics. Note that due to the linearity of the transfer equations, the case of uniform top illumination is obtained by the superposition of such point source solutions.

Using the same cloud as in Fig. 10, Fig. 14a shows the flux pattern for a point source showing that as expected, most of the energy is ultimately reflected. To get a clearer idea of what is going on, we show Figs. 14b and 14c. The dark fractal line leaving from near the source is the division between upward and downward fluxes. All of the downward fluxes originate in the thin white pencil directly below the source. Near the source, the radiation is either left or right in a fairly large region; in the bottom half we see that the flux changes direction frequently and randomly.

Please cite this article in press as: S. Lovejoy, et al., Scattering in thick multifractal clouds, Part II: Multiple scattering, Physica A (2009), doi:10.1016/j.physa.2009.05.037

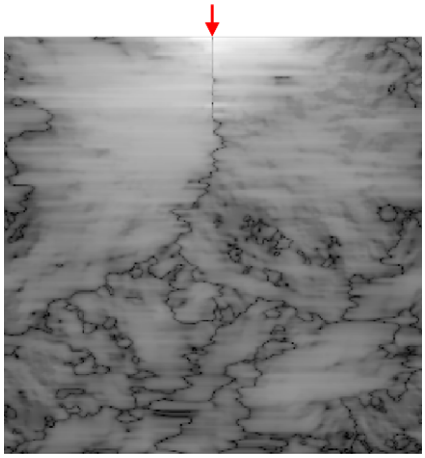

Fig. 14c. Same as Fig. 14b except for the log of the absolute horizontal flux.

7. Conclusion

In terrestrial and astrophysical systems, radiation typically is transported through highly heterogeneous media. Indeed, if we consider turbulence in the broad sense, i.e. including astrophysical MHD turbulence, and in terrestrial atmospheres, multiphase – water/air – and other effects, then radiative transfer applications typically involve turbulent systems (e.g. "clouds"). In the last 20 years it has become increasingly clear that both astrophysical and atmospheric turbulent "clouds" are highly heterogeneous multifractals with interesting, nontrivial, wide range scaling properties ranging over many decades in scale. Unfortunately, with relatively few exceptions, radiative transfer theory has been restricted to plane parallel (or spherically symmetric) geometries wherein horizontal heterogeneity is ignored. The main exceptions to this are purely numerical studies of "3D radiative transfer", typically with relatively thin optical thicknesses so that the effects of heterogeneity are not large. At the same time, the occasional analytic approaches to the problem have been mostly restricted to fairly academic problems such as deterministic monofractal clouds, or to conservative multifractals, or to single scattering.

Recalling the results of Part I of this paper, we showed how our earlier single scattering theory valid for conservative fields can be extended from clouds with analytic scaling exponents (such as "lognormal" multifractals), to clouds with exponents non-analytic at the origin, which describes clouds that are dominated by possibly large and frequently occurring low density regions which are obviously important for the transfer. By developing asymptotic expansions for single scattering cloud statistics in thick clouds, we showed how these holes give increased transmission with qualitatively new (log transmission) behavior while retaining power law terms. We developed an exponent formalism which relates the single scattering photon exponents to the cloud statistical exponents, showing that except for very thick clouds, this power law dominates. Therefore to a first approximation (small κ), this enabled us to "renormalize" the cloud so that the mean cloud transmission is approximately the same as a plane parallel cloud with optical thick thickness $\kappa_{eff} = \kappa^a$; we calculated the exponent a theoretically from the cloud statistics. However two effects cause deviations from this power law renormalization. First, for thick enough clouds the "Lévy hole" power law corrections mentioned above mean that single scattering is ultimately dominated by the holes and so the power law renormalization underestimates the thick cloud single scatter transmission. Second, the total transmission involves multiple scattering, the focus of this part.

In Part II, we quantified the effect of multiple scattering with the help of numerical simulations, showing that the N scattering statistics in a cloud is very nearly given by the theoretical single scattering statistics but for a much thinner cloud: $x_N(\kappa) \approx x_1\left(N^{-1/2}\kappa\right)$ and allowing these "renormalized" single scattering results to be used as approximations to multiple scattering. While this multiple scatter extension of single scatter renormalization is actually quite accurate even in thick clouds, it actually overestimates the transmission. This can seen by the finding that the fractal dimension of photon path walks $D_F > 2$ and slowly increases for large κ; the photon paths are increasingly "subdiffusive". This implies that the scattering locations are increasing clustered, presumably due to "trapping" of photons in optically dense regions. There are thus two opposing effects: the "holes" which lead to increased single scatter transmission and the tendency for multiply scattered photons to become "trapped" in optically dense regions, thus decreasing the overall transmittance. Overall, for "plane parallel" boundary conditions (with a mixture of scattering of all orders) this leads to the renormalization result being reasonably accurate up to $\kappa = 100$ or more (to within 7% for the realistic parameters $\alpha = 1.75$, $H = 0.33$), but with the trapping dominating the effect of holes so that the transmission through the renormalized cloud is a little too high compared to the numerics.

The next step in realism was to extend these results to non-conservative clouds, i.e. those modeled by fractionally integrated turbulent cascades. These are phenomenological models of turbulent fields (when $H = 1/3$ they model passive scalars). In this case, we used numerical methods to show that this single scattering renormalization was still approximately valid even for thick clouds. However realistic systems are superpositions of fields of scattering of many orders, for most

Please cite this article in press as: S. Lovejoy, et al., Scattering in thick multifractal clouds, Part II: Multiple scattering, Physica A (2009), doi:10.1016/j.physa.2009.05.037

problems, it is of interest to solve the radiative transfer equation directly. Since we are only interested in the exponents, we used a numerically efficient sparse matrix method to numerically integrate discrete angle (2D) radiative transfer in which the phase functions consist of four Dirac delta functions at 90°. By varying the extinction coefficient, we are able to study the effect of increasing cloud thickness, for typical cloud mean optical thickness in the range 8–100. For example, using the observed multifractal cloud characteristics, we predict that the mean cloud transmission decreases with the 0.88 power of the total optical thickness (the corresponding homogeneous exponent being unity). For clouds with a total optical thickness of 100 (with $1 - g = 0.15$) this is a non-negligible 35% bias effect with respect to homogeneity with an additional $\pm 25\%$ cloud to cloud variability.

The results in this paper for the first time provide theory applicable to realistic optically thick multifractal clouds. This may have important consequences for estimates of cloud liquid water from satellite observations, and for the handling of radiation in numerical climate models or numerical models of stellar atmospheres. However, we mostly confined our attention to mean "bulk" cloud properties; we did not attempt to relate cloud and radiation fields in a statistical way (at least when multiple scattering is important). Another limitation of the present work is the restriction to isotropic scattering media whereas realistic clouds are highly stratified (although apparently, at least for terrestrial clouds, in a scaling manner). These and other extensions will be the subject for future work.

Acknowledgements

This research was carried out for scientific purposes only, it received no specific funding. We thank P. Gabriel for detailed comments on early drafts of this paper, and we thank A. Davis for useful discussions.

References

[1] M. Lilley, S. Lovejoy, K. Strawbridge, et al., Phys. Rev. E 70 (2004) 036307.
[2] S. Lovejoy, D. Schertzer, M. Lilley, K. Strawbridge, A. Radkevitch, Quart. J. Roy. Meteor. Soc. 134 (2008) 277.
[3] M. Lilley, S. Lovejoy, K. Strawbridge, D. Schertzer, A. Radkevitch, Quart. J. Roy. Meteor. Soc. 134 (2008) 301.
[4] A. Radkevich, S. Lovejoy, K. Strawbridge, D. Schertzer, M. Lilley, Quart. J. Roy. Meteor. Soc. 134 (2008) 316.
[5] S. Lovejoy, D. Schertzer, in: G. Wilkinson (Ed.), Fractals in Geoscience and Remote Sensing, Office for Official Publications of the European Communities, Luxembourg, 1995, p. 102.
[6] A. Davis, A. Marshak, W. Wiscombe, et al., J. Atmos. Sci. 54 (1997) 1423.
[7] K.F. Evans, Geophys. Res. Lett. 20 (1993) 2075.
[8] K.F. Evans, J. Atmos. Sci. 55 (1998) 429.
[9] P.M. Gabriel, S.C. Tsay, G.L. Stephens, J. Atmos. Sci. 50 (1993) 3125.
[10] D.E. Lane-Veron, R.C. Somerville, J. Geophys. Res. 109 (2004) D18113.
[11] R.F. Cahalan, L. Oreopoulos, A. Marshak, et al., Bull. Amer. Meteor. Soc. 86 (2005) 1275.
[12] S. Lovejoy, P. Gabriel, A. Davis, et al., J. Geophys. Res. 95 (1990) 11699.
[13] A. Davis, S. Lovejoy, P. Gabriel, et al., J. Geophys. Res. 95 (1990) 11729.
[14] A. Davis, S. Lovejoy, D. Schertzer, in: S. Keevallik, O. Kärner (Eds.), International Radiation Symposium 92, Deepak, Hampton, Virginia, 1993, p. 112.

Please cite this article in press as: S. Lovejoy, et al., Scattering in thick multifractal clouds, Part II: Multiple scattering, Physica A (2009), doi:10.1016/j.physa.2009.05.037